Autoxidation Chemistry

Bridging the Gap Between Homogeneous Radical Chemistry and (Heterogeneous) Catalysis

Journal Article

Author(s):
Hermans, Ive; Peeters, Jozef; Jacobs, Pierre A.

Autoxidation Chemistry: Bridging the Gap Between Homogeneous Radical Chemistry and (Heterogeneous) Catalysis

Ive Hermans · Jozef Peeters · Pierre A. Jacobs

Abstract During the autoxidation of cyclohexane, abstraction of the αH-atom of the hydroperoxide product by chain-carrying peroxyl radicals produces both the desired alcohol and ketone products, as well as the majority of by-products. Rationalizing the impact of this reaction, one should aim for a (catalytic) destruction of this hydroperoxide without the intervention of peroxyl chain-carriers. Starting from these new insights in the molecular mechanism, attempts for rational catalyst design are initiated.

Keywords Kinetics · Mechanism · Radicals

1 Introduction

Since the middle of the past century, the aerobic oxidation of hydrocarbons has become a major activity in petrochemical industry [1–3]. At present, many large-scale autoxidation processes yield value-added products, using molecular oxygen as the ultimate oxidant. Important examples are the oxidation of cyclohexane to cyclohexanone and cyclohexanol (KA-oil, 10^6 Tons/yr) [4–6], the

I. Hermans · P. A. Jacobs
Department of Microbial and Molecular Systems (M²S), Centre for Surface Chemistry and Catalysis, K. U. Leuven, Kasteelpark Arenberg 23, 3001 Leuven, Belgium

I. Hermans (✉)
Institute for Chemical and Bioengineering, ETH Zürich, Hönggerberg, HCI, Wolfgang-Pauli-Str. 10, 8093 Zurich, Switzerland
e-mail: ive.hermans@chem.ethz.ch

J. Peeters
Department of Chemistry, K. U. Leuven, Celestijnenlaan 200F, 3001 Leuven, Belgium

feedstock chemicals for nylon, and the oxidation of p-xylene to terephthalic acid (3×10^6 Tons/yr), a building block for poly(ethylene terephthalate) [1–3]. A disadvantage of autoxidation chemistry is however that the radical mechanism is often not as selective as desired. This is especially the case for the autoxidation of cyclohexane where the conversion is limited to less than 5% in order to avoid overoxidation of the desired products [1–3], cyclohexyl-hydroperoxide (CyOOH), cyclohexanone (Q=O, where Q denotes $Cy_{-\alpha H}$) and cyclohexanol (CyOH). Indeed, at high conversions, significant amounts of (ring-opened) by-products, such as adipic acid, are formed, lowering the selectivity. Generally spoken, there exist three different strategies for the oxidation of cyclohexane (Scheme 1) [1, 2].
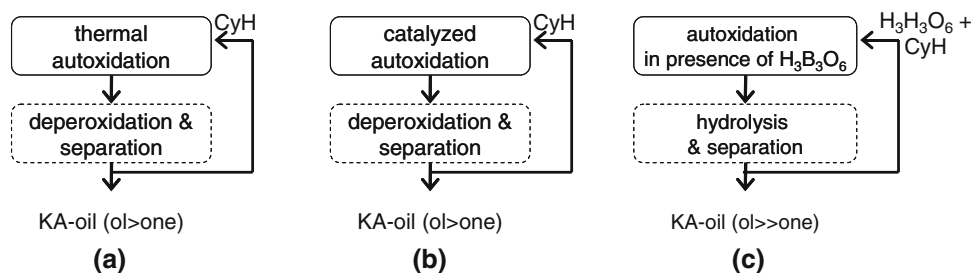
In a first approach (Scheme 1a), cyclohexane is oxidized to a mixture of CyOOH, CyOH and Q=O without a catalyst in a series of agitated reactors at temperatures of 150–180 °C (residence times from 15 to 60 min). The product stream leaving the oxidizers is usually washed with water to remove acidic by-products, followed by a deperoxidation of (remaining) CyOOH to additional CyOH and Q=O with a homogeneous cobalt catalyst. In another approach (Scheme 1b), small amounts (ppb-range) of transition metal salts (e.g. cobalt(II)octanoate) are already added to the oxidation reactor (130–150 °C). Also this approach requires an extensive work-up of the reaction mixture (viz. deperoxidation and separation). Both processes are limited to a conversion of about 5% and produce KA-oil with a ol:one ratio of about 2–3. In the third approach (Scheme 1c), developed in the 1950s by Scientific Design, anhydrous *meta*-boric acid ($H_3B_3O_6$) is added as a slurry to the first oxidation reactor. CyOOH is trapped in situ as the cyclohexyl perborate ester, $B(OOC_6H_{11})_3$. It is further hypothesised that this perborate ester reacts with cyclohexane to yield the borate ester,

Scheme 1 Three different industrial cyclohexane autoxidation strategies

B(OC₆H₁₁)₃, and additional cyclohexanol. The ester is subsequently hydrolyzed to yield cyclohexanol; the boric acid (H_3BO_3) is dehydrated to *meta*-boric acid and recycled (Scheme 1c). The esterification of the hydroperoxide and the alcohol protects them from over-oxidation, and allows the reaction to proceed to higher conversions (10–15%), without loss of a good selectivity (up to $\approx 90\%$, ol:one ≈ 10). Nevertheless, this process suffers from a higher investment and operating cost to recover and recycle the boric acid. At the moment, no heterogeneous-catalyst process is used for the synthesis of KA-oil.

The aim of this paper is to explore new opportunities for autoxidation chemistry, based on some recent advances in the understanding of the radical mechanism. Two recently developed catalytic systems will be reviewed and discussed in the light of the current technology.
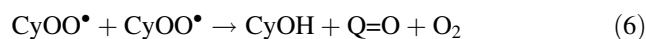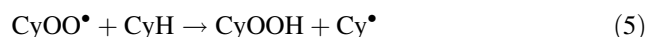
2 The Cyclohexane Autoxidation Mechanism

Despite decades of academic and industrial research, the radical autoxidation mechanism remained poorly understood. It has been assumed that radicals are predominantly generated in the homolytic dissociation of CyOOH (reaction 1), producing cyclohexoxy (CyO$^\bullet$) and hydroxyl ($^\bullet$OH) radicals [1–3]. For this reason, small amounts of CyOOH are often initially added to the feedstock to light off the reaction and avoid an induction period. The CyO$^\bullet$ and $^\bullet$OH oxygen-centered radicals are rapidly converted into carbon-centered radicals upon reaction with the substrate (reactions 2 and 3).

$$CyOOH \rightarrow CyO^\bullet + {}^\bullet OH \tag{1}$$

$$CyO^\bullet + CyH \rightarrow CyOH + Cy^\bullet \tag{2}$$

$$^\bullet OH + CyH \rightarrow H_2O + Cy^\bullet \tag{3}$$

The alkyl free radicals react diffusion-controlled with O_2 to produce the chain carrying peroxyl radicals (reaction 4), able to abstract H-atoms from the substrate (reaction 5). This reaction yields CyOOH and Cy$^\bullet$ radicals which will regenerate peroxyl radicals. The propagation cycle (reactions 4 and 5) is repeated many times before the chain carriers are destroyed in a mutual termination reaction (6).

The *chain length* or average number of propagation cycles between initiation and termination, i.e. the ratio of the propagation and termination rates, is generally accepted to be large, of order of 50 [1–3, 7, 8]. Nevertheless—clearly at odds with the latter—the relatively slow termination (6) and the initiation sequence (1 and 2) were hitherto assumed to be the principal sources of the major "end-"products cyclohexanone and cyclohexanol [1–3]. Yet, this assumption is unable to explain the fairly high yield of CyOH and Q=O relative to the primary product of the propagation reaction (5), CyOOH (Fig. 1).

$$Cy^\bullet + O_2 \rightarrow CyOO^\bullet \tag{4}$$

$$CyOO^\bullet + CyH \rightarrow CyOOH + Cy^\bullet \tag{5}$$

$$CyOO^\bullet + CyOO^\bullet \rightarrow CyOH + Q=O + O_2 \tag{6}$$

Combined experimental and theoretical work of our group revealed that the chain propagating peroxyl radicals not only abstract H-atoms from the substrate, but also, and even much faster, the αH-atoms of the hydroperoxide product [7–9]. A very high ratio of propagation rate constants, $k^{CyOOH}/k^{CyH} \approx 50$ at 145 °C, was theoretically predicted and confirmed by experimental data, identifying CyOOH as a pivotal intermediate in cyclohexane
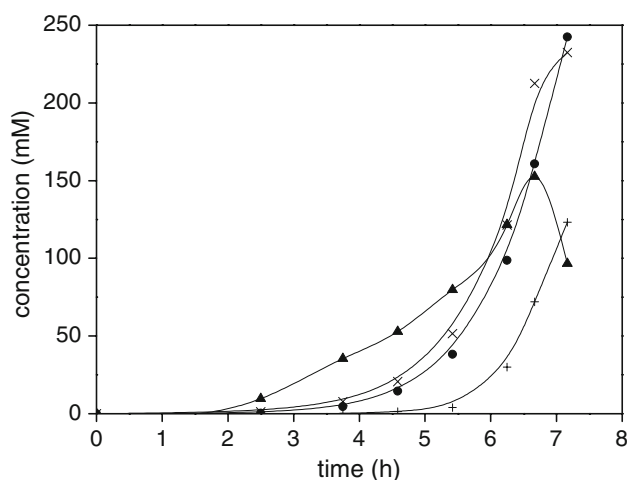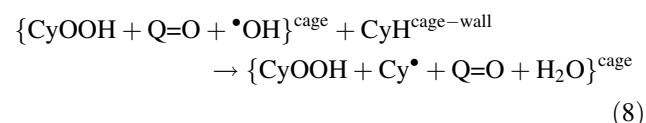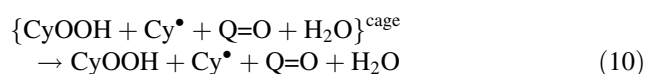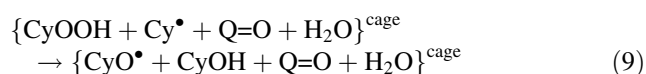

Fig. 1 Evolution of the cyclohexane autoxidation products at 145 °C as a function of time: CyOOH (▲), CyOH (×), Q=O (●), by-products (+)

autoxidation [7, 8]. (Note that all data and values refer to autoxidations at a temperature of 145 °C, unless stated otherwise). Even at a conversion as low as 0.5% (*cfr.* a CyOOH yield of only 35 mM), about 15% of the CyOO$^\bullet$ radicals already react with CyOOH, rather than with CyH. As all radicals of this type [10], the Cy$^\bullet_{-\alpha H}$OOH product is labile and decomposes spontaneously to Q=O and $^\bullet$OH. As a consequence, the mostly overlooked propagation of CyOOH constitutes a fast and straightforward source of cyclohexanone (reaction 7), outrunning Q=O formation via the termination (6) by an order of magnitude (viz. $k^{CyOOH} \times$ [CyOOH]/$k^{term} \times$ [CyOO$^\bullet$] $\approx$ 15 at 1% conversion and 10 at 4% conversion).

$$CyOO^\bullet + CyOOH \rightarrow \{CyOOH + Q=O + {}^\bullet OH\}^{cage} \qquad (7)$$

$$\{CyOOH + Q=O + {}^\bullet OH\}^{cage} + CyH^{cage-wall}$$
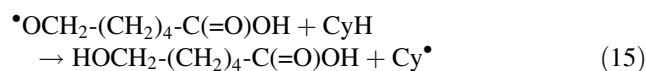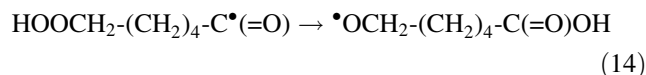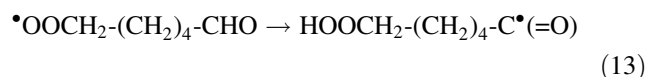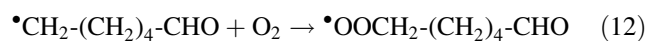$$\rightarrow \{CyOOH + Cy^\bullet + Q=O + H_2O\}^{cage} \qquad (8)$$

The $^\bullet$OH radical is released with a kinetic energy of about 30 kcal/mol and will rapidly abstract an H-atom from a surrounding CyH molecule. This step produces additional heat, making the overall CyOOH propagation exothermic by about 50 kcal/mol. This energy will cause a local activation, or a nano-sized hot-spot, lasting for 10–100 ps and is thus able to steer the fate of the nascent product species [7, 8]. For liquid phase reactions, a fast reaction between nascent reaction products within their common solvent-cage may indeed occur before they diffuse away from each other. For the system at issue, cage-reaction (9), is greatly speed up by the 50 kcal/mol cage-activation, and can compete with the out-of-cage diffusion (10), which is only slightly promoted by thermal activation because of a smaller energy barrier.

$$\{CyOOH + Cy^\bullet + Q=O + H_2O\}^{cage}$$
$$\rightarrow \{CyO^\bullet + CyOH + Q=O + H_2O\}^{cage} \qquad (9)$$

$$\{CyOOH + Cy^\bullet + Q=O + H_2O\}^{cage}$$
$$\rightarrow CyOOH + Cy^\bullet + Q=O + H_2O \qquad (10)$$

Kinetic and stoichiometric analyses of the experimental data reveal that the reactive flux going to the $\{CyO^\bullet + CyOH + Q=O + H_2O\}$ products constitutes about 70% [8]. Note that this cage-channel causes a net destruction of CyOOH, explaining why this product features a maximum as a function of time (Fig. 1). At this CyOOH maximum, the CyOOH formation rate ($k^{CyH} \times$ [CyH]) should equal the CyOOH removal rate ($k^{CyOOH} \times$ [CyOH] $\times$ cage-fraction), from which k^{CyOOH} is indeed found one order of magnitude larger than k^{CyH}. Reaction (9) produces not only CyOH, but also CyO$^\bullet$, part of which is converted to CyOH via reaction (2). Another and even slightly more important pathway for CyO$^\bullet$ at 145 °C, is the unimolecular β C–C cleavage (11), yielding ring-opened ω-formyl radicals [11].

$$CyO^\bullet \rightarrow {}^\bullet CH_2\text{-}(CH_2)_4\text{-}CHO \qquad (11)$$

These ω-formyl radicals are rapidly converted to 6-hydroxyhexanoic acid (reactions 12–15), experimentally identified as the most important precursor of other by-products [12].

$${}^\bullet CH_2\text{-}(CH_2)_4\text{-}CHO + O_2 \rightarrow {}^\bullet OOCH_2\text{-}(CH_2)_4\text{-}CHO \qquad (12)$$

$${}^\bullet OOCH_2\text{-}(CH_2)_4\text{-}CHO \rightarrow HOOCH_2\text{-}(CH_2)_4\text{-}C^\bullet(=O) \qquad (13)$$

$$HOOCH_2\text{-}(CH_2)_4\text{-}C^\bullet(=O) \rightarrow {}^\bullet OCH_2\text{-}(CH_2)_4\text{-}C(=O)OH \qquad (14)$$

$${}^\bullet OCH_2\text{-}(CH_2)_4\text{-}C(=O)OH + CyH$$
$$\rightarrow HOCH_2\text{-}(CH_2)_4\text{-}C(=O)OH + Cy^\bullet \qquad (15)$$

This implies that the majority of by-products ($\geq$80%) stems from CyOOH rather than Q=O ($\leq$20%), [8, 12] contrary to earlier literature assumptions [1–3]. This is in accord with the rate constant ratio of the respective CyOO$^\bullet$ reactions: $k^{Q=O}/k^{CyOOH}$ is found to be only $\approx$ 0.1.
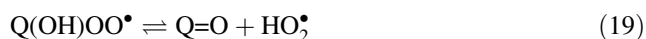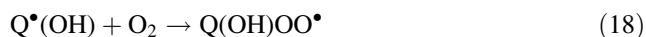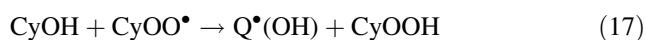
On the other hand, the crucial role of Q=O in the chain-initiation was long overlooked. It should first be stressed that the homolytic dissociation of CyOOH (reaction 1) is not only very slow, due to the 40 kcal/mol energy barrier, but also highly inefficient in the liquid phase as the nascent CyO$^\bullet$ and $^\bullet$OH radicals will much faster undergo geminate recombination than diffuse away from each other [13]. Recently, we discovered and kinetically quantified a much faster and more efficient initiation mechanism of CyOOH, assisted by Q=O. In this reaction (16), the $^\bullet$OH radical breaking away from a partially dissociated CyO–OH molecule abstracts a weakly bonded αH-atom of Q=O, producing the resonance-stabilized ketonyl radical plus CyO$^\bullet$ hydrogen-bonded to water [13].

$$CyOOH + Q=O \rightarrow CyO^\bullet \cdots H_2O + Q^\bullet_{-\alpha H}=O \qquad (16)$$
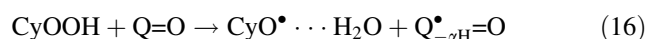
The energy barrier for this reaction (viz. 27.7 kcal/mol) is much lower than that for the simple homolysis (1). Furthermore, the probability for geminate recombination of the radicals from reaction (16) is strongly reduced by various stabilization effects [13]. As increasing amounts of ketone are produced during cyclohexane autoxidation (Fig. 1), the rate of initiation reaction (16) increases rapidly, causing the observed autocatalytic upswing (Fig. 1).

Co-oxidation of CyOH by CyOO$^\bullet$-attack proceeds preferably via the abstraction of the αH-atom (reaction 17, $k^{CyOH}/k^{CyH} \approx$ 10). The α-hydroxy-alkyl-peroxyl radicals resulting from subsequent O$_2$ addition (reaction 18) decompose very rapidly to HO$_2^\bullet$ + Q=O via equilibrium (19), which is strongly shifted towards the right by the entropic effect, despite its endothermicity of $\approx$ 15 kcal/mol [7, 8, 14]. This decomposition of Q(OH)OO$^\bullet$ far outruns its hitherto

accepted bimolecular reactions with e.g. CyH or CyOO$^{\bullet}$ (20 and 21).

$$CyOH + CyOO^{\bullet} \rightarrow Q^{\bullet}(OH) + CyOOH \qquad (17)$$

$$Q^{\bullet}(OH) + O_2 \rightarrow Q(OH)OO^{\bullet} \qquad (18)$$

$$Q(OH)OO^{\bullet} \rightleftharpoons Q{=}O + HO_2^{\bullet} \qquad (19)$$

$$Q(OH)OO^{\bullet} + CyH \rightarrow Q(OH)OOH + Cy^{\bullet} \qquad (20)$$

$$Q(OH)OO^{\bullet} + CyOO^{\bullet} \rightarrow Q(OH)O^{\bullet} + CyO^{\bullet} + O_2 \qquad (21)$$

HO$_2^{\bullet}$ radicals can abstract H-atoms from the substrate (reaction 22) and produce H_2O_2, experimentally observed during CyH autoxidation [15]. But, more importantly for the mechanism, HO$_2^{\bullet}$ can also react with peroxyl radicals in a diffusion controlled head-to-tail termination reaction (23) [16]. Therefore, the co-oxidation of CyOH will slow down the overall oxidation rate.

$$HO_2^{\bullet} + CyH \rightarrow H_2O_2 + Cy^{\bullet} \qquad (22)$$

$$CyOO^{\bullet} + HO_2^{\bullet} \rightarrow CyOOH + O_2 \qquad (23)$$
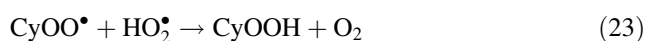
According to this revised autoxidation scheme, alcohol, ketone, as well as the majority of by-products originate from the fast co-propagation of the hydroperoxide product. The propagation of CyOH, although slower than that of CyOOH, is responsible for a slight decrease of the reaction rate, due to the formation of chain-terminating HO$_2^{\bullet}$ radicals. On the other hand, cyclohexanone assists in the formation of new radicals, whereas overoxidation of this product is relatively slow. Note that this mechanism readily explains why the CyH conversion can be increased in the boric-acid modified process, without a significant increase in by-products. Indeed, esterification of CyOOH with $H_3B_3O_6$ to the cyclohexylperborate ester lowers its reactivity towards the peroxyl radicals by steric hindrance, preventing the formation of a large quantity of cyclohexoxy radicals which yield by-products (reactions 12–15). These new insights also hold important clues for the design of (alternative) catalytic processes. Indeed, one could not only reduce the reactivity of CyOOH towards the peroxyl radicals as one does in the boric acid process, one could also aim for a fast catalytic decomposition of this intermediate, preventing it to react with CyOO$^{\bullet}$.

3 Catalysis by Immobilized Cr Colloids

Whereas cobalt and manganese ions are only able to catalyze the chain initiation via a Haber–Weiss cycle (Scheme 2), chromium ions are additionally able to catalyze the dehydration of hydroperoxides [1, 2]. This transition element could thus achieve an in situ deperoxidation towards the most desired product, cyclohexanone.

A disadvantage of chromium is however its noxious nature, especially of Cr(VI) [17]. Therefore, immobilization of the
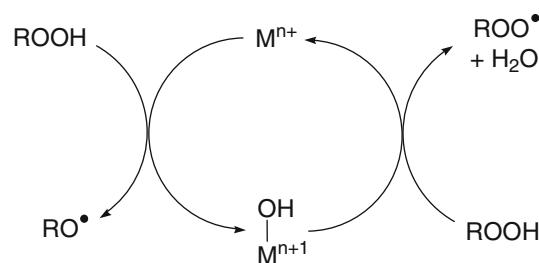
Scheme 2 Haber–Weiss catalytic cycle for $M^{n/n+1}$ transition metal ions: enhancement of the initiation rate

chromium active sites is an important prerequisite for the large-scale application of this element. In the nineties, many attempts were made to synthesize a stable heterogeneous Cr catalyst, but, unlike cobalt, the incorporation of chromium in the framework of (micro) porous materials seems less evident [18]. Indeed, under autoxidation conditions nearly all of them suffer from severe leaching [19]. Specifically for the classical CrAlPO$_4$-5, experimental evidence was provided that the Cr would not be incorporated into the framework, but be present as octahedral ions at the surface of the zeolite crystals [20]. This way, Cr might be leached easily, assisted by complexation by reaction products. This instability does not only contaminate the product stream, it also limits the lifetime of the solid catalyst. However, more recently, a stable incorporation of Cr^{3+} in the AlPO$_4$-5 framework became possible with a new synthesis procedure [21–23].

Alternatively, and inspired by the low solubility of Cr(III)oxide, we recently developed a new immobilization strategy, based on the precipitation of Cr colloids on inert support material [24, 25]. This technique produces highly dispersed nano-sized Cr(III)oxide particles with a high catalytic activity. In this approach, Cr(III) colloids are generated upon slow addition of $K_2Cr_2O_7$ (1–5 μmol/min) to a stirred reactor, containing an aqueous solution of hydrazine (0.1 M). During the fast reduction reaction, the Cr ions are hydrolyzed, triggering their polymerization to nano-sized colloids as witnessed by Dynamic Light Scattering (DLS) [24, 25]. As Ca^{2+} ions can stabilize the negatively charged colloids, and SO_4^{2-} ions assist in the hydrolysis reaction, $CaSO_4$ was added to the system to facilitate colloid formation and deposition [24]. The content of the reactor is continuously pumped over a chromatographic column, packed with support material (e.g. silica gel) on which the Cr particles are partially immobilized via precipitation. A positive correlation between the Cr-loading and the average pore size of the support material is observed when dosing the same total amount of Cr(VI) [25]. This observation is in disagreement with the hypothesis of ion-exchange being the dominant immobilization mechanism. Colloid precipitation can however readily explain such a correlation as particles are deposited more easily on widely accessible surfaces, i.e.
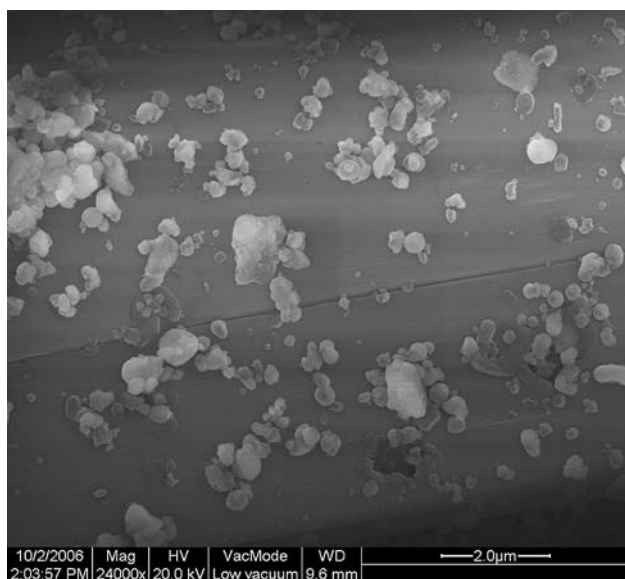
Fig. 2 SEM picture of Cr(III)colloids at the external surface of a silica support particle (reproduced by permission of the PCCP owner societies) [25]

on the walls of large pores and to the external surface. The proposed deposition mechanism is in line with the XPS and EDX characterization of the solid materials, demonstrating an enrichment of Cr at the external surface of the particles. With SEM, Cr containing particles can indeed be observed sticking to the surface of the support (Fig. 2).

These observations for colloid-deposited samples are significantly different from those for classically impregnated materials which show a homogeneous Cr-distribution over the support particles as capillary forces ensure evenly filled pores [25]. Clearly there is a distinct physico-chemical difference between impregnation, ion-exchange and colloid precipitation as an immobilization strategy. It was additionally observed that the amount of Cr which can be immobilized on a given support depends on the concentration and the rate at which the Cr(VI) is dosed to the system. This effect should be ascribed to an increase in particle size as observed by DLS: although the immobilization (filtration) efficiency of the chromatographic column is nearly insensitive to the particle size in the 1–1,000 nm range [26], withdrawing of larger particles results in a higher Cr loading. Apparently, the faster Cr(VI) is dosed to the immobilization system, and/or the higher its concentration, the larger the Cr particles become, and the more Cr can be loaded onto the support. TEM reveals that the larger Cr particles are composed of smaller building blocks of about 10 nm in size (Fig. 3) [25], the reason being that the growth of the elementary colloids is kinetically unfavourable, compared to their aggregation. The size of such secondary particles depends on the concentration of building blocks and can be tuned by changing the Cr(VI) concentration and dosing rate.
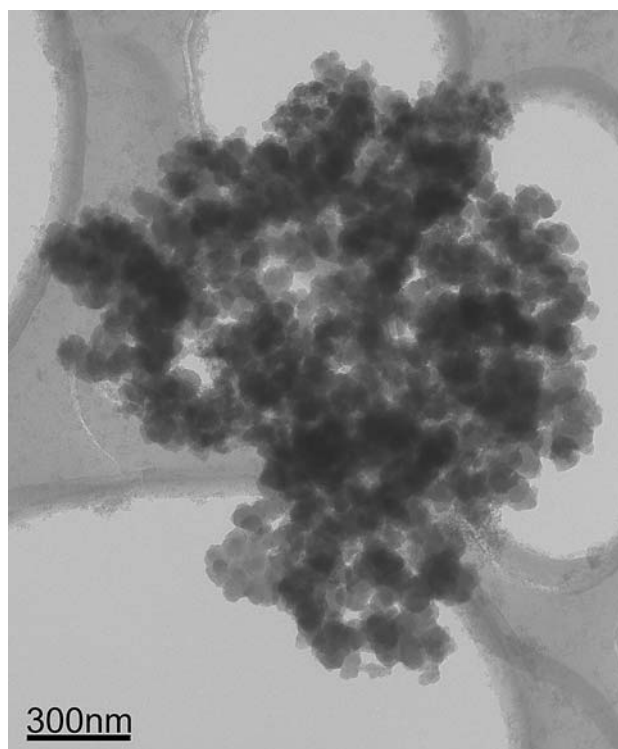

Fig. 3 TEM picture of a Cr colloid, composed of smaller building block units of about 10 nm in size (reproduced by permission of the PCCP owner societies) [25]

The impact of $CaSO_4$ and/or other salts on the size and morphology of the (secondary) particles is currently under investigation. It is expected that the added salt, as well as the used solvent(-composition), are important parameters which can be used to synthesize custom-made immobilized colloids tailored to specific needs, not only from chromium, but also from other metals.

The autoxidation of cyclohexane in the presence of such immobilized Cr particles was studied at 130 °C [24]. Whereas at this temperature it takes the non-catalyzed system about 19 h to reach 3% conversion, 5 ppm of a 13.0 mg Cr/g colloid-based catalyst achieves this conversion in about 2.5 h. When comparing the product distribution of such a catalyzed reaction (Fig. 4) with that of a thermal autoxidation (Fig. 5), one observes that even this small amount of catalyst is able to achieve a nearly complete deperoxidation and to increase the Q=O yield significantly. Although the by-products also increase upon addition of the chromium catalyst, one should realize that if one would aim for the same degree of deperoxidation via radical pathways, the amount of by-products would be significantly higher. Probably, the high Q=O yield causes this increase in by-products. Figure 6 shows the product distribution obtained with 5 ppm of a conventional homogeneous Co(acac)$_2$ catalyst. Apparently also this catalyst produces more by-products than the thermal system, although with an one:ol ratio of only 0.7–1,
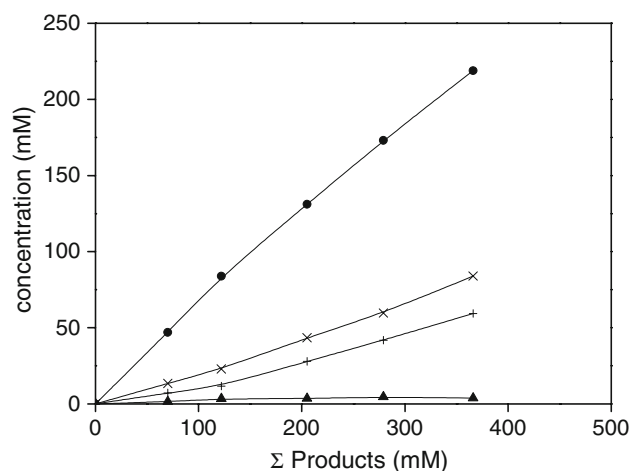
Fig. 4 Product distribution during the 130 °C autoxidation of cyclohexane in the presence of 5 ppm Cr (13.0 mg Cr/g); CyOOH (▲), CyOH (×), Q=O (•), by-products (+)
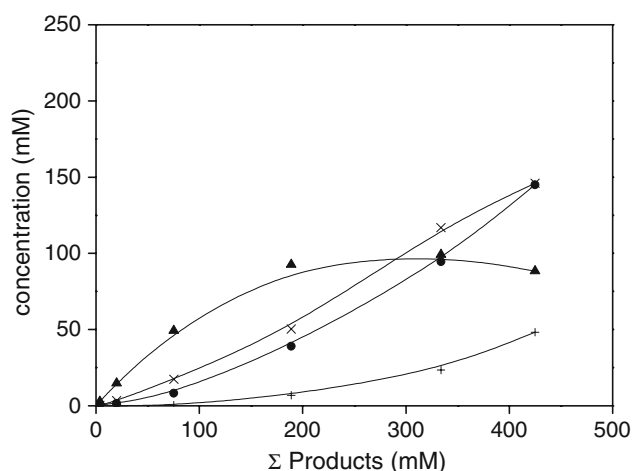

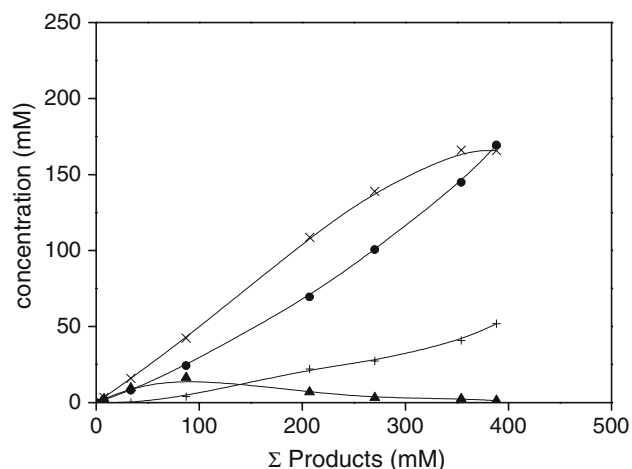**Fig. 5** Product distribution during the 130 °C autoxidation of cyclohexane; CyOOH (▲), CyOH (×), Q=O (•), by-products (+)

Fig. 6 Product distribution during the 130 °C autoxidation of cyclohexane in the presence of 5 ppm Co(acac)$_2$; CyOOH (▲), CyOH (×), Q=O (•), by-products (+)

compared to ≈ 2.6 for the heterogeneous Cr system. The increase in by-products in this system should be ascribed to the production of a large amount of CyO$^\bullet$ radicals in the reaction of CyOOH with the Co^{2+} (Scheme 2). The immobilized colloids clearly result in a favourable ketone/by-product ratio.

The stability of the colloid based catalyst was studied under batch conditions and strong evidence was provided for the heterogeneous nature of the catalysis [24]. For instance, analysis of the liquid phase with Atomic Absorption Spectroscopy could not reveal any Cr in solution (leaching below 2 ppb detection limit). Moreover, the oxidation activity of the liquid phase, separated from the solid catalyst above room temperature to avoid the re-adsorption of potentially leached species, was found identical to a mixture containing the same quantities of products, but devoid of Cr. This is in sharp contrast with the situation encountered with impregnated CrCl$_3$ catalysts where all Cr immediately leaches to the liquid phase, causing homogeneous, rather than heterogeneous catalysis. An EXAFS study should provide more information on the atomic environment of the Cr centres and identify the molecular differences between the new colloidal system and impregnated samples. If this catalyst also maintains its stability in a continuous flow reactor, as it does under batch conditions, the separate deperoxidation step could be eliminated. Additionally, this colloid immobilization strategy should be explored also for other metal oxides as it provides an elegant way to synthesize supported nano-catalysts.

4 Catalysis by Inert H-bond Acceptors

During the main stage of the autoxidation reaction, radicals are generated via initiation reaction (16). However, at low conversion, i.e. where little Q=O has been produced yet, the initiation proceeds via the significantly slower reaction (24), the rate constant of which is 1,000 times smaller than of reaction (16) [13].

$$CyOOH + CyH \rightarrow CyO^\bullet \cdots H_2O + Cy^\bullet \qquad (24)$$
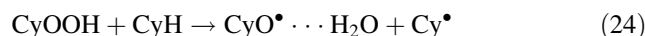
Therefore, addition of a compound which could promote initiation at low conversion could significantly reduce the induction period. It was rationalized that (inert) H-bond accepters (X) could fulfill this role as they can stabilize the $^\bullet$OH radical breaking away from CyO–OH, not via the formation of H$_2$O as in reactions (16) and (24), but via the formation of an H-bonded complex (reaction 25).

$$CyOOH + X \rightarrow CyO^\bullet + {}^\bullet OH \cdots X \qquad (25)$$

This complex (X$\cdots^\bullet$OH) will decompose thermally to X plus $^\bullet$OH, closing a catalytic cycle. This concept was experimentally confirmed by the observation that addition of

1 vol% of CH_3CN, H_2O and HOAc significantly accelerates the cyclohexane autoxidation, although these compounds are no radical sources themselves [27]. The activity-order $CH_3CN \leq H_2O < HOAc$ follows the computed trend in H-bond strengths between these molecules and the $^\bullet OH$ radical (i.e. 4.4, 4.4 and 6.4 kcal/mol, respectively). These observations prompted us to investigate the opportunities of a new type of organo-catalyst for cyclohexane autoxidation.

It was found that inert perfluorinated compounds such as perfluorodecaline (PFD) and Teflon are rather efficient autoxidation catalysts, not only reducing the timescale of the oxidation (e.g. time to reach 3.6% conversion reduced from 20 h to 13 h in presence of 0.5 vol% PFD at 130 °C), but also improving the product distribution [27]. For instance at 145 °C, it was found that 5 w% of Teflon powder (1 μm) induced a shift in product distribution from 26.5, 33.0 and 32.5% of Q=O, CyOH, and CyOOH, respectively to 54.0, 28.0 and 10.0%, respectively at 4% conversion. Apparently, Teflon causes a significant decrease in the CyOOH yield, associated with an increase in the Q=O yield. Similar results were observed with PFD and should probably be ascribed to a catalyzed CyOOH propagation. Indeed, perfluorinated compounds can form two H-bonds with the H-abstraction TS of reaction (7) whereas only one is possible with the CyOOH reactant. Therefore the barrier of this reaction will be reduced upon addition of such a multiple H-bond acceptor. Note that such a catalyzed propagation is less likely for CyH as this molecule is not an H-bond donor as CyOOH, reducing the probability to find a perfluorinated compound in the vicinity of the TS for H-abstraction reaction (2). Therefore the k^{CyOOH}/k^{CyH} ratio will be enhanced, leading not only to an absolute, but also a relative increase in the CyOOH propagation, explaining the observed changes in CyOOH and Q=O yield. A similar behavior was recently also observed by others, studying the catalytic oxidation of cyclohexene in PFD [28]. The reason why CyOH does not increase, as one would expect at first sight, but even decreases, should also be ascribed to the H-bonding effect. Indeed, the "hot" $^\bullet OH$ radical expelled by the $Cy_{-\alpha H}{}^\bullet OOH$ radical in reaction (7) will also be stabilized by the inert H-bond acceptor. Such an interaction will lower the instantaneous heat-release by reaction (8) following the CyOOH propagation (7). As this heat is crucial to render the subsequent cage-reaction (9) competitive with out-diffusion (10), one can indeed understand the decrease in CyOH yield in these catalyzed reactions [27]. Fluorous biphasic systems thus offer interesting opportunities to improve autoxidation chemistry without major changes to the current industrial set-up, although optimization could obviate a harsh deper-oxidation step.

References

1. Sheldon RA, Kochi JK (1981) Metal-catalyzed oxidations of organic compounds. Academic Press, New York
2. Franz G, Sheldon RA (2000) In: Ullmann's encyclopedia of industrial chemistry. Wiley-VCH, Weinheim
3. Bhaduri S, Mukesh D (2000) Homogeneous catalysis, mechanisms and industrial applications. John Wiley & Sons, New York
4. Musser MT (2000) In: Ullmann's encyclopedia of industrial chemistry. Wiley-VCH, Weinheim
5. Berezin IV, Denisov ET, Emanuel NM (1966) The oxidation of cyclohexane. Pergamon Press, Oxford
6. Schuchardt U, Cardoso D, Sercheli R, Pereira R, da Cruz RS, Guerreiro MC, Mandelli D, Spinacé EV, Pires EL (2001) Appl Catal A: Gen 211:1
7. Hermans I, Nguyen TL, Jacobs PA, Peeters J (2005) ChemPhysChem 6:637
8. Hermans I, Jacobs PA, Peeters J (2006) J Mol Catal A: Chem 251:221
9. Hermans I, Peeters J, Jacobs P (2007) J Org Chem 72:3057
10. Vereecken L, Nguyen TL, Hermans I, Peeters J (2004) Chem Phys Lett 393:432
11. Beckwith ALJ, Hay BP (1989) J Am Chem Soc 111:2674
12. Hermans I, Jacobs PA, Peeters J (2007) Chem Eur J 13:754
13. Hermans I, Jacobs PA, Peeters J (2006) Chem Eur J 12:4229
14. Hermans I, Müller J-F, Nguyen TL, Jacobs PA, Peeters J (2005) J Phys Chem A 109:4303
15. Tolman CA, Druliner JD, Nappa MJ, Herron N (1989) In: Hill CL (ed) Activation and functionalization of alkanes. John Wiley & Sons, New York, p 303
16. Rowley DM, Lesclaux R, Lightfoot PD, Nozière B, Wallington TJ, Hurley MD (1992) J Phys Chem 96:4889
17. Weckhuysen BM, Wachs IE, Schoonheydt RA (1996) Chem Rev 96:3327
18. (a) Rajic N, Stojakovic D, Hocevar S, Kaucic V (1993) Zeolites 13:384; (b) Weckhuysen BM, Schoonheydt RA (1994) Stud Surf Sci Catal 14:360; (c) Demuth D, Unger KK, Schuth F, Stucky GD, Srdanov VI (1994) Adv Mater 6:931; (d) Demuth D, Unger KK, Schuth F, Srdanov VI, Stucky GD (1995) J Phys Chem 99:479; (e) Weckhuysen BM, Schoonheydt RA, Mabbs FE, Collison D (1996) J Chem Soc, Faraday Trans 92:2431; (f) Chen JD, Lempers HEB, Sheldon RA (1996) J Chem Soc, Faraday Trans 92:1807; (g) Radaev SF, Joswig W, Baur WHJ (1996) Mater Chem 6:1413; (h) Thiele S, Hoffman K, Vetter R, Marlow F, Radaev S (1997) Zeolites 19:190; (i) Zhu ZD, Wasowicz T, Kevan L (1997) J Phys Chem B 101:10763; (j) Zhu ZD, Kevan L (1999) Phys Chem Chem Phys 1:199; (k) Miyake M, Uehara H, Suzuki H, Yao ZD, Matsuda M, Sato M (1999) Microporous Mesoporous Mater 32:45; (l) Prakash AM, Hartmann M, Zhu ZD, Kevan L (2000) J Phys Chem B 104:1610
19. (a) Sheldon RA, Wallau M, Arends IWCE, Schuchardt U (1998) Acc Chem Res 31:485; (b) Lempers HEB, Sheldon RA (1998) J Catal 175:62
20. Weckhuysen BM, Schoonheydt RA (1994) Zeolites 14:360
21. (a) Kornatowski J, Zadrozna G, Wloch J, Rozwadowski M (1999) Langmuir 15:5863; (b) Padlyak BV, Kornatowski J, Zadrozna G, Rozwadowski M, Gutsze A (2000) J Phys Chem A 104:11837; (c) Kornatowski J, Zadrozna G, Rozwadowski M, Zibrowius B, Marlow F, Lercher JA (2001) Chem Mater 13:4447; (d) Zadrozna G, Souvage E, Kornatowski J (2002) J Catal 208:270
22. Laha SC, Kamalakar G, Gläser R (2006) Micro Meso Mat 90:45

23. Baele AM, Grandjean D, Kornatowski J, Glatzel P, de Groot FMF, Weckhuysen BM (2006) J Phys Chem B 110:716

24. Breynaert E, Hermans I, Lambie B, Maes G, Peeters J, Maes A, Jacobs P (2006) Angew Chem Int Ed 45:7584

25. Hermans I, Breynaert E, Poelman H, De Gryse R, Liang D, Van Tendeloo G, Maes A, Peeters J, Jacobs P (2007) Phys Chem Chem Phys 9:5382

26. Breynaert E, Maes A (2005) Anal Chem 77:5048

27. Hermans I, Jacobs PA, Peeters J (2006) Chem Phys Chem 7:1142

28. de Castries A, Magnier E, Monmotton S, Fensterbank H, Larpent C (2006) Eur J Org Chem 20:4685